IKR Publishers

IKR Journal of Agriculture and Biosciences
(IKRJAB)
Journal homepage: https://ikrpublishers.com/ikrjab/
Volume-1, Issue-4 (November-December) 2025
OPEN ACCESS
ISSN: 3107-5509 (Online)

Oxidative Stress and Haematological Alterations in Wistar Rats Exposed to Polluted and Phytoremediated Ubeji River Water

Bello-Adedipe, Zuleihat Ohunene[1] & Adeyemi, Olalekan[1,2*]

[1]Department of Environmental Management and Toxicology, Federal University of Petroleum Resources, Effurun, Delta State
[2]Department of Biochemistry, Federal University of Petroleum Resources, Effurun, Delta State

DOI:*10.5281/zenodo.17845189*

ARTICLE INFO

Article history:
Received : 17-11-2025
Accepted : 24-11-2025
Available online : 07-12-2025

Copyright©2025 The Author(s): This is an open-access article distributed under the terms of the Creative Commons Attribution **4.0 International License (CC BY-NC)** which permits unrestricted use, distribution, and reproduction in any medium for non-commercial use provided the original author and source are credited.

Citation: Bello-Adedipe, Z. O., & Adeyemi, O. (2025). Oxidative Stress and Haematological Alterations in Wistar Rats Exposed to Polluted and Phytoremediated Ubeji River Water. *IKR Journal of Agriculture and Biosciences (IKRJAB)*, 1(4), 238-254.

ABSTRACT **Original Research Article**

This study aimed to evaluate the haematological, biochemical, and antioxidant alterations resulting from graded exposure to polluted river water and to determine the potential health risks associated with such contamination, while also assessing the ameliorative potential of phytoremediated water from *Eichhornia crassipes*. Wistar rats were exposed for 28 days to different concentrations of polluted water (100%, 75%, 50%, 25%), phytoremediated water, and a clean-water control. Haematological indices, serum lipid profile, and oxidative stress biomarkers were quantified using standard automated and spectrophotometric methods. Significant haematological disruptions ($p < 0.05$) were observed in exposed groups. White blood cell counts increased markedly, with Group A recording 12.8×10^9/L compared with 6.55×10^9/L in the control ($p < 0.05$). Red cell parameters declined progressively, with Group A showing the lowest RBC (5.5×10^{12}/L), HGB (9.75 g/dL), and HCT (30.55%), indicating pollutant-induced anaemia. Serum lipid analyses revealed dyslipidaemia ($p < 0.05$): LDL peaked in Group D, HDL was highest in Group A, triglycerides increased significantly in Group A relative to the control ($p < 0.05$), and total cholesterol was highest in Group D. Oxidative stress biomarkers also varied significantly across tissues. MDA levels were elevated in Group B liver, Group C kidney, and Group A serum (all $p < 0.05$). Antioxidant responses showed non-linear modulation: hepatic GSH was highest in Group A, renal GSH lowest in Group B ($p < 0.05$), GST activity peaked in Group B stomach and colon ($p < 0.05$), and catalase induction was strongest in Group A kidney ($p < 0.05$). Serum and colonic SOD were significantly reduced in exposed groups ($p < 0.05$). Notably, rats exposed to phytoremediated water showed improved haematological stability, moderated lipid disruptions, and enhanced antioxidant responses compared with those exposed to untreated polluted water, indicating partial detoxification resulting from phytoremediation. In conclusion, polluted river water caused significant haematotoxicity, dyslipidaemia, and oxidative imbalance, demonstrating organ-specific susceptibility, while phytoremediation using *Eichhornia crassipes* provided measurable mitigation. It is recommended that routine monitoring, phytoremediation-based remediation, and community sensitisation be prioritised to mitigate associated health risks.

Keywords: Polluted River Water, Oxidative Stress, Haematotoxicity, Antioxidant Enzymes, Dyslipidaemia.

**Corresponding author: Adeyemi, Olalekan*
Department of Biochemistry, Federal University of Petroleum Resources, Effurun, Delta State

Introduction

Freshwater ecosystems across the Niger Delta have experienced decades of cumulative degradation arising from oil exploration, petrochemical discharge, artisanal refining, and poorly regulated industrial activities. These stressors have resulted in severe declines in water quality, with pollutants such as heavy metals, polycyclic aromatic hydrocarbons (PAHs), suspended solids, and complex organic mixtures being routinely recorded in impacted rivers (Aigbedion & Chukwuma, 2024; Edokpa et al., 2023; Oghenevwairhe et al., 2023). Ubeji River, situated downstream of the Warri Refining and Petrochemical Company (WRPC), represents one of the most chronically affected water bodies, with repeated

reports of effluent discharge, black-soot fallout, and hydrocarbon contamination. These pollutants often persist, bioaccumulate, and exert toxicological effects on aquatic organisms and humans residing within surrounding communities (Ede et al., 2020; Pakuła et al., 2021). Chronic exposure to such complex pollutant mixtures poses significant ecological and public-health concerns, particularly in regions where river systems serve as primary water sources for domestic, agricultural, and recreational activities.

Experimental toxicology studies increasingly demonstrate that contaminated surface waters trigger profound biochemical, haematological, and oxidative alterations in mammals. Pollutant-laden waters are known to induce leukocytic activation, erythrocyte suppression, membrane fragility, and metabolic derailment, often mediated through oxidative stress pathways (Omoregie & Ekpo, 2020; Musa et al., 2022). Hydrocarbons, phenolic compounds, metals, and other effluent-derived xenobiotics disrupt cellular redox balance by generating reactive oxygen species (ROS) that overwhelm antioxidant defences, leading to lipid peroxidation, protein modification, and DNA instability (Li et al., 2022; Zhao et al., 2022). Biomarkers such as malondialdehyde (MDA), glutathione (GSH), catalase (CAT), superoxide dismutase (SOD), and glutathione-S-transferase (GST) therefore serve as critical indicators of pollutant-induced oxidative injury and tissue susceptibility. Similarly, haematological indices—including RBC, WBC, HGB, HCT, and differential leukocyte counts—provide sensitive, early-warning signals of immunotoxicity, anaemia, and systemic physiological stress (Rahman et al., 2022).

Rivers impacted by petrochemical activities are additionally associated with disruptions in lipid metabolism, evidenced by pollutant-induced dyslipidaemia that manifests as altered LDL, HDL, triglycerides, and total cholesterol profiles (Adebayo et al., 2021; Olayinka et al., 2022). These biochemical disturbances heighten risks of cardiovascular dysfunction and systemic metabolic imbalance in exposed populations. Given the established vulnerability of freshwater systems in the Niger Delta, and the increasing reliance of surrounding communities on these water resources, there is a pressing need to characterise the toxicological consequences of exposure to polluted river water using relevant mammalian models.

This study therefore evaluates the haematological, biochemical, and oxidative stress responses of Wistar rats following graded exposure to polluted water from Ubeji River. Using a 28-day exposure model, the research investigates dose-dependent alterations in blood indices, lipid profile, and antioxidant biomarkers—providing a comprehensive assessment of the systemic and organ-specific toxicological effects of contaminated surface water. The findings contribute critical evidence toward understanding pollutant-mediated physiological disruption and underscore the broader implications for environmental health and community safety in petroleum-impacted regions.

Materials and Methods

Study Area and Polluted Water Source

Polluted river water was collected from a designated point along a chronically impacted Ubeji River, located downstream of the Warri Refining and Petrochemical Company (WRPC), Delta State, Nigeria (Adeyemi & Bello-Ogundipe, 2025). Sampling was carried out at midstream to ensure representative pollutant load. Water samples were collected in pre-acid-washed 2 L amber glass bottles, transported on ice to the laboratory, and stored at 4 °C prior to use. All handling followed standard procedures for water-sample preservation according to APHA (2022).

Experimental Animals and Ethical Approval

Thirty healthy adult male Wistar rats (180–220 g) were procured from a certified animal breeding facility. Animals were acclimatised for 14 days under standard laboratory conditions (22 ± 2 °C; 12 h light/dark cycle; relative humidity 55–65%). Rats were fed commercial grower pellets and provided water *ad libitum*. All procedures involving animals were conducted in accordance with institutional ethical guidelines and approved by the University Animal Care and Use Committee, following the principles of the National Research Council (2020).

Experimental Design and Water Exposure Regimen

Animals were randomly assigned into five groups (n = 6 per group) as follows:

- **Group A (100%)** – Full-strength polluted river water
- **Group B (75%)** – 75% polluted water + 25% clean water
- **Group C (50%)** – 50% polluted water + 50% clean water
- **Group D (25%)** – 25% polluted water + 75% clean water
- **Group E (Control)** – 100% clean borehole/distilled-quality water

Exposure lasted 28 consecutive days, during which rats received only the assigned water concentrations for drinking. Daily observations were conducted to monitor behaviour, food and water intake, and signs of toxicity.

Haematological Analysis

At the end of the exposure period, rats were fasted overnight and anaesthetised with ketamine/xylazine (80/10 mg/kg i.p.).

Blood was collected via cardiac puncture into EDTA-coated tubes for haematological assays. Parameters including WBC, RBC, HGB, HCT, MCV, MCHC, PLT, and differential leukocyte counts were determined using an automated haematology analyser (Sysmex XP-300, Kobe, Japan). Procedures followed standard methods outlined by Dacie and Lewis (2021).

Serum Biochemical Assays

Lipid Profile Determination

Blood collected into plain tubes was allowed to clot and centrifuged at 3,500 rpm for 10 minutes. Serum concentrations of LDL, HDL, triglycerides, and total cholesterol were quantified using enzymatic colorimetric diagnostic kits (Randox Laboratories Ltd., UK) according to manufacturer protocols (Salah & Ahmed, 2021).

Tissue Collection and Homogenate Preparation

Following euthanasia, the liver, kidneys, stomach, and colon were harvested, rinsed in ice-cold physiological saline, blotted dry, and weighed. Each tissue was homogenised in ice-cold 0.1 M phosphate buffer (pH 7.4) using a Teflon-glass homogeniser. Homogenates were centrifuged at 10,000 rpm for 15 minutes at 4 °C, and the supernatants were collected for oxidative stress assays. All procedures followed the method described by Buege and Aust (2020).

Oxidative Stress Biomarker Assays

Malondialdehyde (MDA) Assay

Lipid peroxidation was measured using the thiobarbituric acid reactive substances (TBARS) method. MDA concentrations were quantified spectrophotometrically at 532 nm and expressed as nmol MDA/mg protein (Ohkawa et al., 2020).

Reduced Glutathione (GSH) Assay

GSH levels were determined using the Ellman method, involving reaction with 5,5'-dithiobis-(2-nitrobenzoic acid) (DTNB). Absorbance was measured at 412 nm, and concentrations expressed as µmol GSH/mg protein (Sedlak & Lindsay, 2021).

Glutathione-S-Transferase (GST) Activity

GST specific activity was assessed using 1-chloro-2,4-dinitrobenzene (CDNB) as substrate, following the method of Habig and Jakoby (2020). Enzyme activity was recorded at 340 nm and expressed as U/mg protein.

Catalase (CAT) Activity

CAT activity was determined based on the decomposition of hydrogen peroxide, monitored at 240 nm according to the Aebi (2021) method. Activities were expressed as U/mg protein.

Superoxide Dismutase (SOD) Activity

SOD activity was estimated by inhibition of pyrogallol auto-oxidation at 420 nm following Marklund and Marklund (2020). Activities were expressed as U/mg protein.

Protein Quantification

Tissue protein concentration was determined using the Bradford (1976) method with bovine serum albumin as standard.

Statistical Analysis

All data were expressed as mean ± standard error of mean (SEM). Statistical analyses were performed using SPSS version 25.0. One-way analysis of variance (ANOVA) was used to determine differences among groups, followed by Tukey's post-hoc test for multiple comparisons. Statistical significance was accepted at $p < 0.05$. Graphical presentations were produced using GraphPad Prism version 9.0.

Results

The haematological profile of rats exposed to different concentrations of polluted river water (Groups A–D) compared with the control (Group E) (Table 1) reveals clear dose-dependent alterations in blood parameters.

White blood cell (WBC) counts were significantly elevated in Group A (12.8×10^9/L) compared with the control (6.55×10^9/L), suggesting immune activation and systemic stress due to exposure to untreated polluted water. Conversely, red blood cell (RBC), haemoglobin (HGB), and haematocrit (HCT) values showed a consistent decline from the control to the highly exposed group, with the lowest values observed in Group A (RBC: 5.5×10^{12}/L; HGB: 9.75 g/dL; HCT: 30.55%). This indicates impaired erythropoiesis or possible haemolysis under pollutant stress.

Indices such as mean corpuscular volume (MCV) and mean corpuscular haemoglobin concentration (MCHC) remained largely stable across groups, though Group E had slightly lower MCV, reflecting no drastic shifts in red cell size or haemoglobin concentration per cell. Platelet (PLT) counts increased significantly with decreasing exposure, ranging from 605×10^9/L in Group A to 965×10^9/L in Group E, suggesting suppression of thrombopoiesis in heavily polluted groups.

Neutrophil (NEU) percentages were highest in Group A (38.1%) and lowest in the control (25.75%), confirming an inflammatory response to polluted water. Conversely, lymphocyte (LYM) percentages showed the opposite trend, being lowest in Group A (56.1%) and highest in the control (69.55%), indicating a shift in leukocyte distribution under stress. Eosinophils (EOS) followed a similar declining trend, while monocytes (MON) remained relatively stable across groups. Basophils (BASO) showed negligible changes.

Overall, these results demonstrate that polluted river water caused immune stimulation, anaemia, and haematological imbalances in a concentration-dependent manner, with Group A showing the most severe alterations. This indicates toxic stress and impaired haematopoietic function due to pollutant exposure.

Table 1: Haematological Profile of Rats Exposed to Different Concentrations of Polluted River Water (Mean ± SEM)

Parameter	A (±SEM)	B (±SEM)	C (±SEM)	D (±SEM)	E (±SEM)
WBC (×10⁹/L)	12.8 ± 0.3 a	11.0 ± 0.2 ab	8.8 ± 0.2 bc	7.35 ± 0.15 cd	6.55 ± 0.15 d
RBC (×10¹²/L)	5.5 ± 0.1 e	6.05 ± 0.05 d	6.75 ± 0.05 c	7.35 ± 0.05 b	8.35 ± 0.15 a
HGB (g/dl)	9.75 ± 0.15 e	11.0 ± 0.1 d	12.1 ± 0.1 c	13.15 ± 0.05 b	14.15 ± 0.15 a
HCT (%)	30.55 ± 0.45 e	33.75 ± 0.25 d	37.35 ± 0.15 c	40.9 ± 0.1 b	43.6 ± 0.4 a
MCV (fL)	55.6 ± 0.2 ab	55.75 ± 0.05 a	55.35 ± 0.65 ab	55.65 ± 0.25 a	52.25 ± 0.45 b
MCHC (g/dL)	31.95 ± 0.05 b	32.55 ± 0.15 a	32.2 ± 0.1 ab	32.4 ± 0.1 ab	32.45 ± 0.05 a
PLT (×10⁹/L)	605 ± 15 e	710 ± 10 d	775 ± 5 c	865 ± 5 b	965 ± 15 a
NEU (%)	38.1 ± 0.6 a	33.85 ± 0.65 b	30.3 ± 0.2 c	27.85 ± 0.25 cd	25.75 ± 0.35 d
LYM (%)	56.1 ± 0.4 e	60.85 ± 0.65 d	64.75 ± 0.25 c	67.45 ± 0.35 b	69.55 ± 0.55 a
EOS (%)	2.2 ± 0.1 a	1.9 ± 0.1 ab	1.8 ± 0.1 bc	1.55 ± 0.05 cd	1.45 ± 0.05 d
MON (%)	3.0 ± 0.2 b	3.4 ± 0.1 a	3.15 ± 0.05 ab	3.15 ± 0.15 ab	3.2 ± 0.3 ab
BASO (%)	0.1 ± 0.1	0.0 ± 0.0	0.0 ± 0.0	0.0 ± 0.0	0.1 ± 0.0

The serum lipid profiles of rats exposed to different concentrations of polluted river water (Figures 1a–d) reveal statistically significant differences both when compared with the control and among the treatment groups ($p < 0.05$).

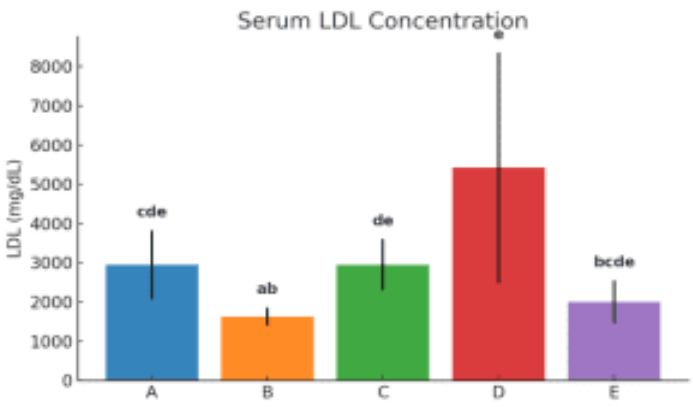
In **Figure 1a (LDL concentration)**, Group D (25% exposure) recorded the highest LDL level, which was significantly higher ($p < 0.05$) than Groups B and E, and also distinct from Groups A and C as indicated by non-overlapping superscripts. Groups A and C showed intermediate but significantly elevated LDL compared with Group B. The lowest LDL was observed in Group B, which was statistically similar to the control but significantly lower than Groups A, C, and D. This shows that LDL increase followed a non-linear trend, with Group D being most affected.

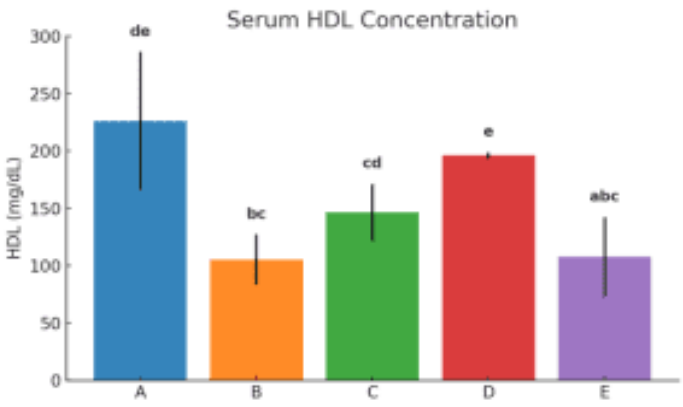
Figure 1b (HDL concentration) showed Group A (100%) as having the highest HDL, significantly greater ($p < 0.05$) than Groups B, C, and E. Group D also had elevated HDL, significantly higher than Groups B and E. By contrast, Groups B and E recorded the lowest HDL values, which were not significantly different from each other but significantly lower than Groups A and D. This indicates that while heavy exposure (100%) and moderate exposure (25%) increased HDL, intermediate exposures led to depressed HDL levels.

In **Figure 1c (Triglycerides concentration)**, Group A displayed the highest triglyceride level, significantly greater ($p < 0.05$) than all other groups. Groups B, C, and D had statistically similar values, but all were higher than the control (E). The control recorded the lowest triglycerides, significantly different from Group A but overlapping with B–D. This shows a concentration-dependent effect, with full exposure causing hypertriglyceridaemia.

Figure 1d (Total cholesterol concentration) revealed Group D as having the highest concentration, significantly higher ($p < 0.05$) than all other groups. Groups A and C showed moderate cholesterol levels, significantly higher than Groups B and E but lower than Group D. Group B and the control had the lowest cholesterol, with no significant difference between them. Thus, Group D demonstrated the most severe hypercholesterolaemia.

Overall interpretation: Significant differences ($p < 0.05$) were observed both between the exposed groups and when compared to the control. Group D showed the most severe dyslipidaemia, with the highest LDL and total cholesterol. Group A exhibited hypertriglyceridaemia and elevated HDL, suggesting compensatory stress responses. Groups B and E consistently maintained the lowest lipid values, with no significant difference between them, while Group C remained intermediate. These results confirm that polluted river water exposure disrupts lipid homeostasis in a concentration-dependent but non-linear manner, predisposing exposed rats to cardiovascular and metabolic risks.





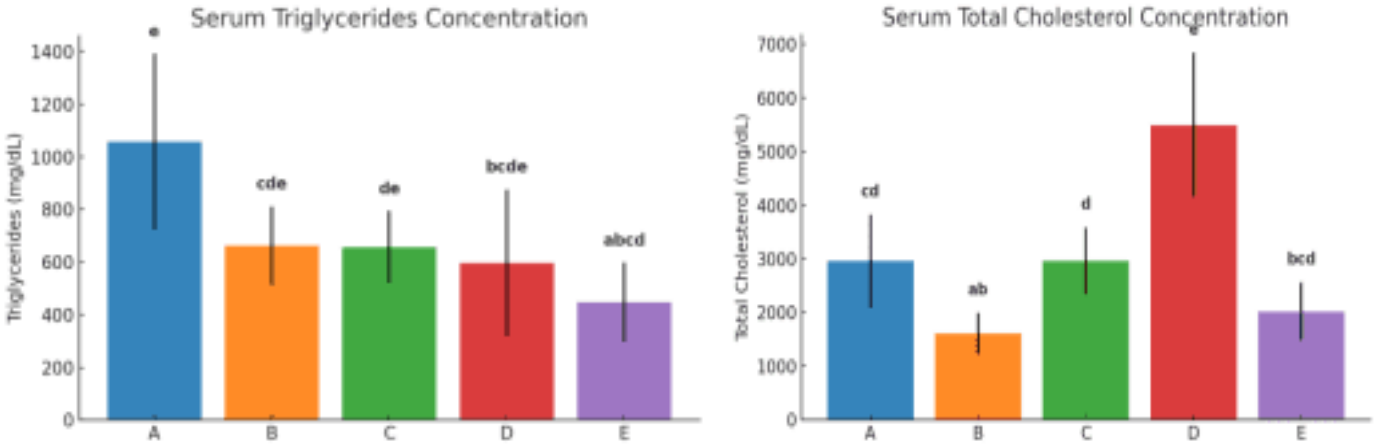


Figure 1: Serum Lipid Profiles (LDL, HDL, Triglycerides, and Total Cholesterol) of Rats Exposed to Different Concentrations of Polluted River Water (Mean ± SEM, $p < 0.05$)

Figure 2 presents the malondialdehyde (MDA) concentrations in the liver, kidney, stomach, colon, and serum of rats exposed to various concentrations of polluted river water. The results reveal significant tissue-specific and concentration-dependent alterations in oxidative stress biomarkers ($p < 0.05$).

In the **liver**, Group B recorded the highest MDA concentration, significantly higher ($p < 0.05$) than Group A, with Groups D and E also elevated. Group A showed the lowest value, indicating that full-strength exposure (100%) did not cause the highest lipid peroxidation, but rather intermediate exposure increased oxidative stress.

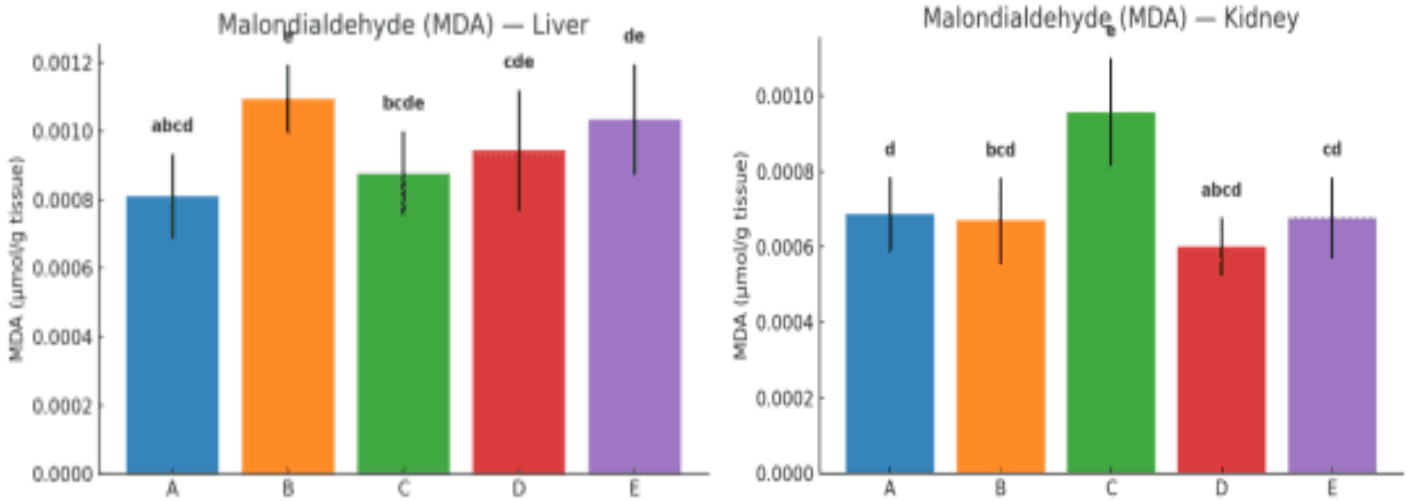
For the **kidney**, Group C exhibited the highest MDA level, significantly higher than all other groups, while Group D showed the lowest concentration. This suggests that moderate exposure triggered greater oxidative stress in renal tissues than either full or diluted exposures, pointing to a non-linear response.

In the **stomach**, Group B again showed the highest MDA concentration, significantly greater ($p < 0.05$) than Groups A, D, and E. The lowest values were recorded in Groups D and E, while Group A had moderate levels. This indicates that intermediate exposure most strongly promoted lipid peroxidation in gastric tissue.

The **colon** results showed Group E (control) with the highest MDA concentration, followed by Group B. Groups A, C, and D were significantly lower ($p < 0.05$). The elevated control value may suggest baseline oxidative activity or adaptive suppression of peroxidation in exposed groups.

In the **serum**, Group A displayed the highest MDA concentration, significantly greater ($p < 0.05$) than Groups C and D, with Group C showing the lowest value. Groups B and E remained intermediate. This indicates that systemic oxidative stress was strongest in rats exposed to full-strength polluted water.

Overall interpretation: The data demonstrate that MDA levels varied significantly across tissues and exposure groups ($p < 0.05$). While serum and kidney tissues showed peak oxidative stress at 100% and 50% exposures respectively, stomach and liver tissues responded most strongly at 75%. The colon presented an unusual trend, with the control group having the highest values. These findings indicate that oxidative stress induced by polluted river water is both tissue-specific and non-linear, reflecting complex interactions between pollutant concentration, tissue susceptibility, and adaptive responses.



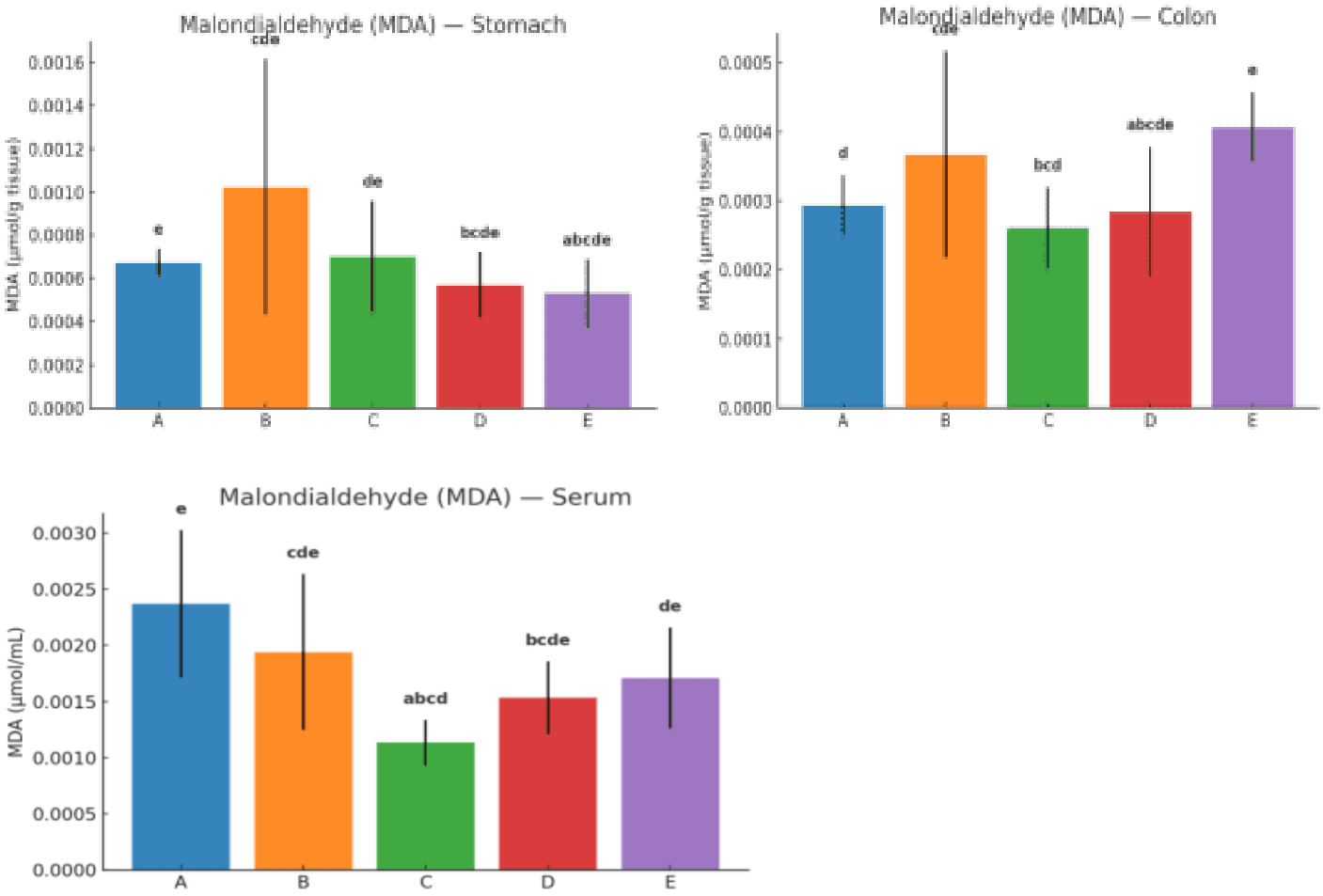


Figure 2: Malondialdehyde (MDA) Concentrations in Liver, Kidney, Stomach, Colon, and Serum of Rats Exposed to Different Concentrations of Polluted River Water (Mean ± SEM, $p < 0.05$)

Figure 3 shows the reduced glutathione (GSH) concentrations in the liver, kidney, stomach, colon, and serum of rats exposed to varying concentrations of polluted river water. The results highlight significant tissue-specific and dose-dependent variations ($p < 0.05$) in antioxidant status.

In the **liver**, Group A (100%) exhibited the highest GSH concentration, significantly higher ($p < 0.05$) than all other groups. GSH levels declined progressively across Groups B, C, and D, with Group D showing the lowest concentration. The control group (E) showed moderate levels, lower than Group A but higher than Groups C and D. This suggests that high pollutant exposure triggered an adaptive upregulation of hepatic GSH, while prolonged or intermediate exposures depleted reserves.

For the **kidney**, Groups D and E recorded the highest GSH values, significantly higher ($p < 0.05$) than Groups A, B, and C. Group B showed the lowest concentration, with significant reductions compared with all other groups. These results suggest that moderate to no exposure favoured renal antioxidant defence, while intermediate exposures depleted renal GSH.

In the **stomach**, Group A had the highest GSH concentration, significantly higher than all other groups. The lowest levels were observed in Groups C and E, with Group B showing moderate depletion. This indicates that the stomach responded strongly to high pollutant exposure by increasing GSH, possibly as a defence against oxidative injury.

In the **colon**, GSH levels were relatively stable across all groups, with only slight variations. Group B showed the highest value, significantly different from Group A, while the control (E) also had relatively elevated concentrations. This suggests that colonic GSH was less sensitive to pollutant concentration, maintaining near-steady levels.

In the **serum**, Group E (control) had the highest GSH concentration, significantly higher ($p < 0.05$) than all other groups, followed by Group D. Groups A, B, and C displayed lower values, with Group B being the lowest. This indicates systemic antioxidant depletion under pollutant stress, with preservation in the unexposed control.

Overall interpretation: GSH responses were tissue-dependent and non-linear. In liver and stomach tissues, full exposure (Group A) enhanced GSH levels as a compensatory mechanism, whereas in the kidney and serum, GSH was best preserved in the control and moderately exposed groups. The colon showed minimal variation. These findings indicate that polluted river water induced oxidative stress that altered glutathione metabolism differently across tissues, reflecting varying antioxidant defence capacities and susceptibilities ($p < 0.05$).

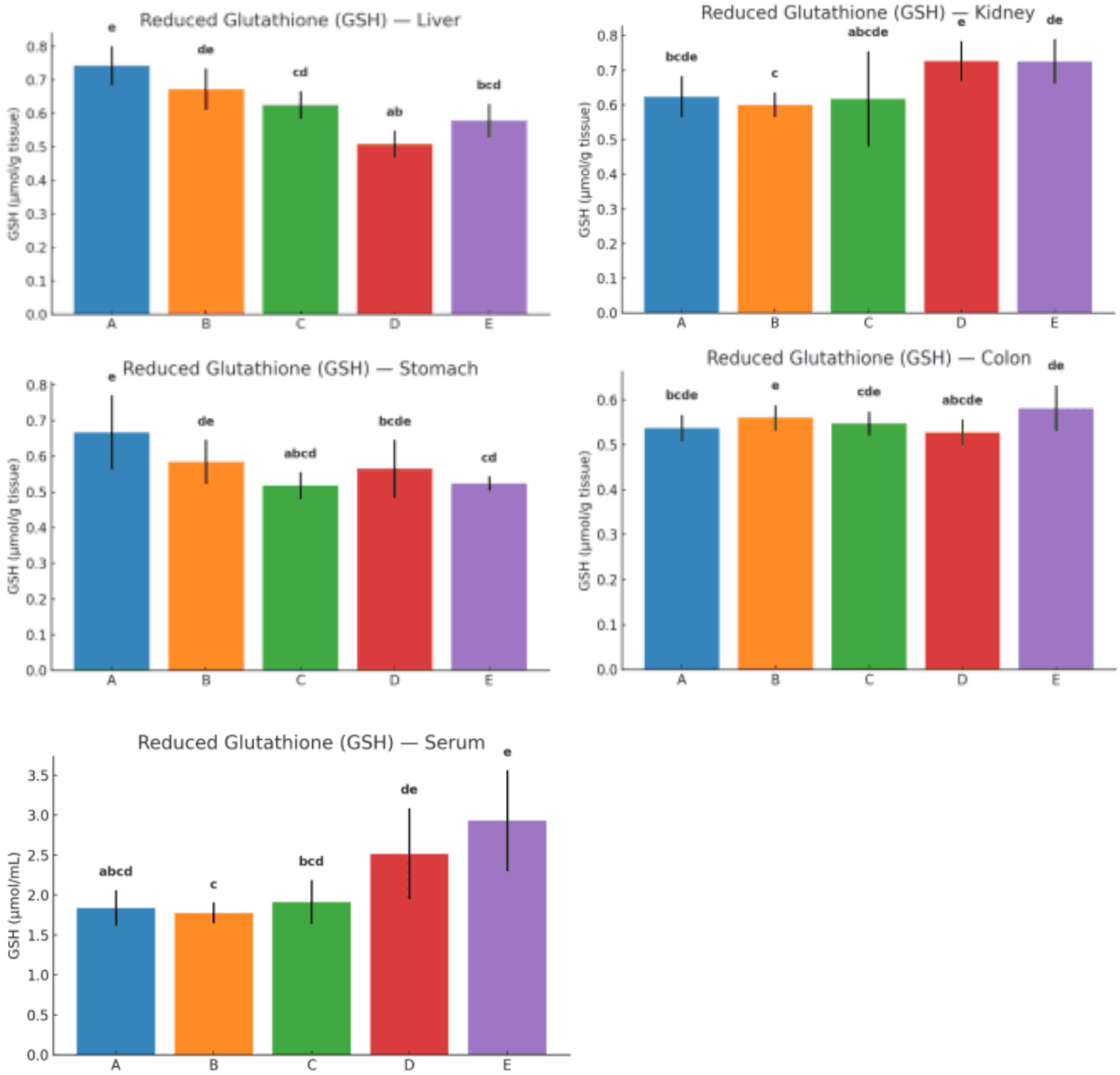


Figure 3: Reduced Glutathione (GSH) Concentrations in Liver, Kidney, Stomach, Colon, and Serum of Rats Exposed to Different Concentrations of Polluted River Water (Mean ± SEM, $p < 0.05$)

Figure 4 presents the glutathione-S-transferase (GST) specific activity in the liver, kidney, stomach, colon, and serum of rats exposed to various concentrations of polluted river water. The results show tissue-specific differences and statistically significant variations among groups ($p < 0.05$).

In the **liver**, GST activity was relatively stable across all groups, with no significant differences ($p > 0.05$). This suggests that hepatic GST activity was not markedly influenced by pollutant exposure, possibly reflecting the liver's strong baseline detoxification capacity.

For the **kidney**, Group A (100%) showed the highest GST activity, significantly greater ($p < 0.05$) than all other groups. Group D also recorded elevated activity compared with B, C, and E. The lowest activity was observed in the control (E), significantly different from Group A. This indicates pollutant-induced upregulation of renal GST at high exposure levels, suggesting adaptive detoxification responses.

In the **stomach**, Group B exhibited the highest GST activity, significantly higher ($p < 0.05$) than all other groups. Group C followed, while Groups A, D, and E recorded significantly lower activities. This marked elevation in Group B suggests strong induction of gastric GST at moderate exposure, possibly reflecting heightened detoxification activity at this dose.

The **colon** showed peak GST activity in Group B, significantly greater ($p < 0.05$) than Groups C, D, and E.

Group A also recorded high activity but was lower than Group B. Groups D and E had the lowest activities, with no significant difference between them. This indicates that colonic GST was most responsive at moderate exposure.

In the **serum**, Group D had an exceptionally high GST activity, significantly greater ($p < 0.05$) than all other groups by a wide margin. Groups A, B, C, and E recorded very low activities, with the control (E) being the lowest. The dramatic increase in Group D suggests systemic induction of GST at 25% exposure, pointing to a strong but non-linear detoxification response.

GST activity was tissue-dependent and non-linear across exposure groups ($p < 0.05$). While liver activity remained stable, the kidney and stomach showed significant induction at high and moderate exposures, respectively. The colon responded maximally at moderate exposure (Group B), while serum GST activity spiked dramatically in Group D. These results suggest that polluted river water induces detoxification responses differently across tissues, with GST activity reflecting the interplay between pollutant concentration and tissue-specific adaptive capacity.

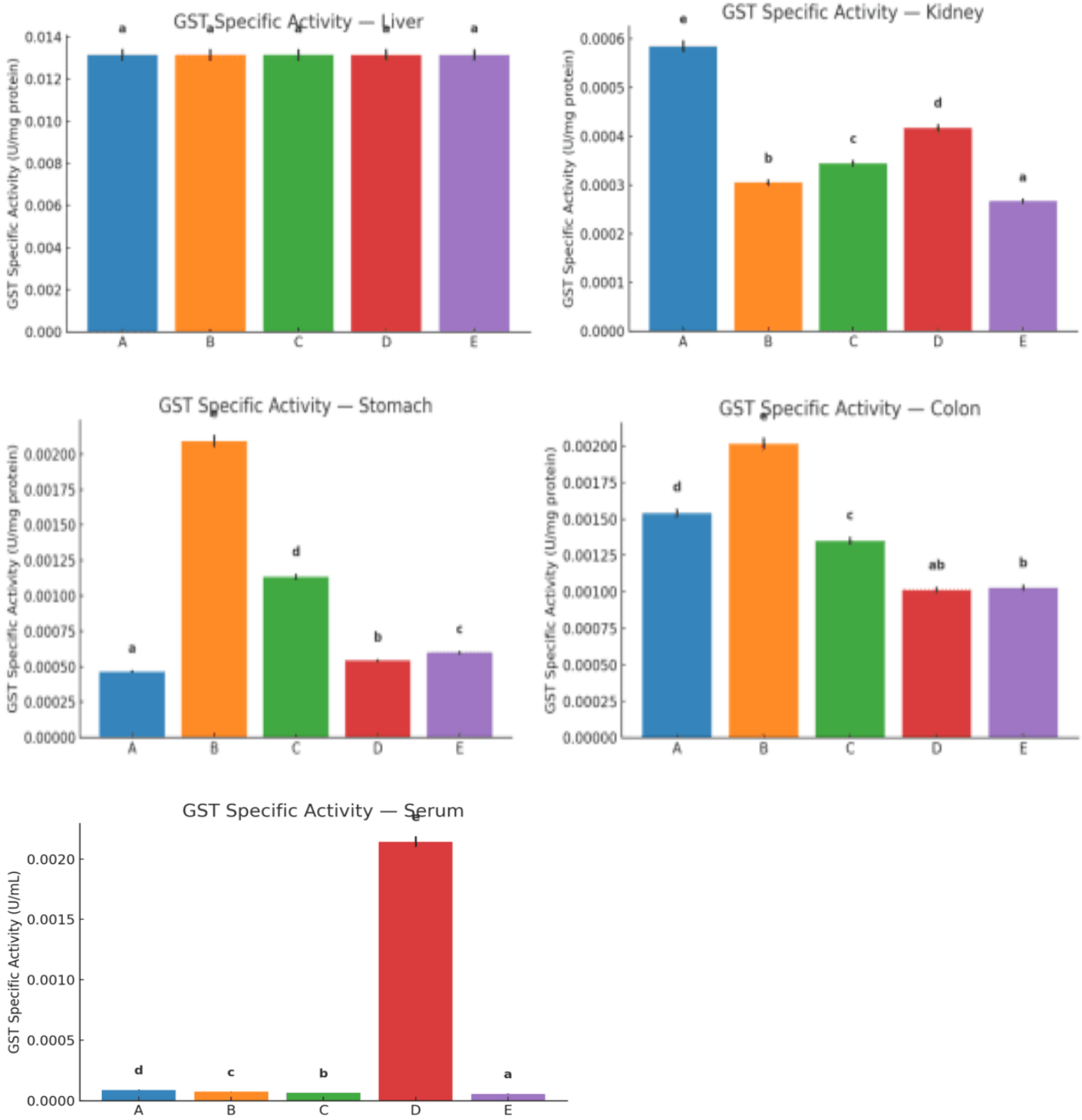


Figure 4: Glutathione-S-Transferase (GST) Specific Activity in Liver, Kidney, Stomach, Colon, and Serum of Rats Exposed to Different Concentrations of Polluted River Water (Mean ± SEM, $p < 0.05$)

Figure 5 shows catalase (CAT) activity in the liver, kidney, stomach, colon, and serum of rats exposed to varying concentrations of polluted river water. The results highlight significant tissue-specific variations and concentration-dependent responses ($p < 0.05$).

In the **liver**, CAT activity remained stable across all groups, with no significant differences ($p > 0.05$). This suggests that hepatic catalase was unaffected by pollutant exposure, likely due to the liver's strong baseline antioxidant defence capacity.

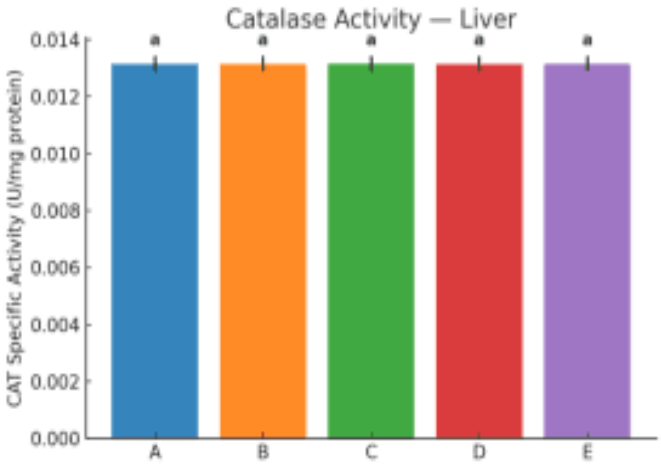
For the **kidney**, Group A (100%) exhibited the highest CAT activity, significantly greater ($p < 0.05$) than all other groups. Group B followed, while Groups C and D had moderate activity, and the control (E) recorded the lowest value. This pattern indicates that pollutant exposure strongly induced renal catalase activity, reflecting oxidative stress adaptation at higher exposure levels.

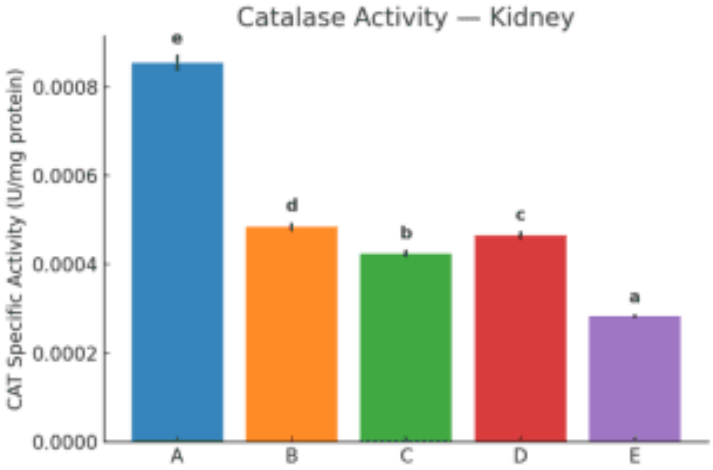
In the **stomach**, catalase activity was uniform across all groups, showing no significant differences ($p > 0.05$). This suggests that stomach catalase remained unaffected by pollutant concentration, possibly due to alternative antioxidant mechanisms compensating for oxidative stress.

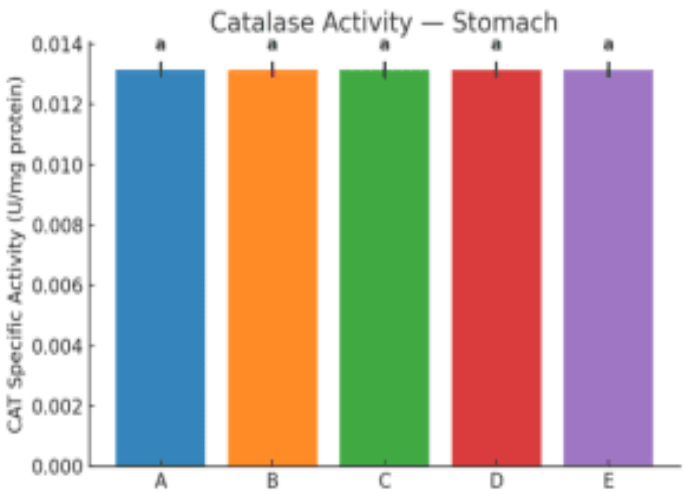
The **colon** displayed the highest CAT activity in Group B, which was significantly higher ($p < 0.05$) than all other groups. Group A followed, while Groups C and D showed moderate activity. The control group (E) had the lowest catalase levels. This suggests that moderate pollutant exposure triggered strong colonic catalase induction, while absence of pollutants maintained baseline activity.

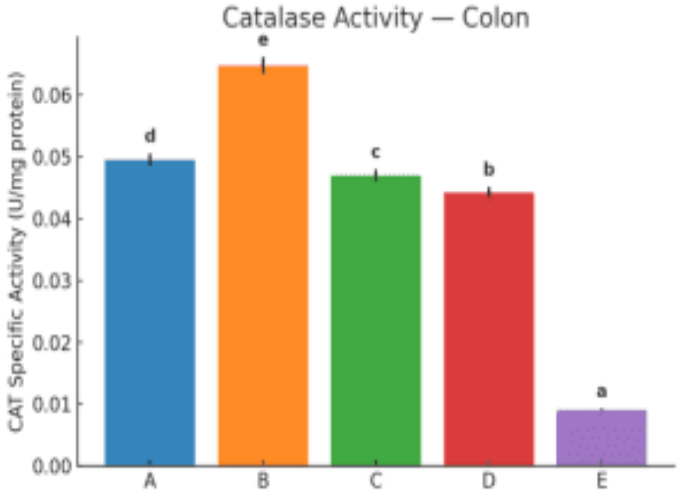
In the **serum**, the control group (E) exhibited the highest CAT activity, significantly greater ($p < 0.05$) than all exposed groups. Group D also showed relatively high levels, followed by Group A. Groups B and C recorded the lowest activities, with Group C being significantly reduced. These results suggest systemic catalase depletion under pollutant exposure, with preserved activity only in unexposed controls.

CAT activity showed tissue-dependent and concentration-specific responses ($p < 0.05$). The liver and stomach maintained stable catalase activity irrespective of exposure, whereas the kidney and colon exhibited strong induction at high and moderate exposures, respectively. Serum catalase, however, was highest in the control and reduced in exposed groups, indicating systemic oxidative stress. These findings demonstrate that polluted river water induces non-linear and tissue-specific catalase responses, reflecting varied antioxidant defence capacities.









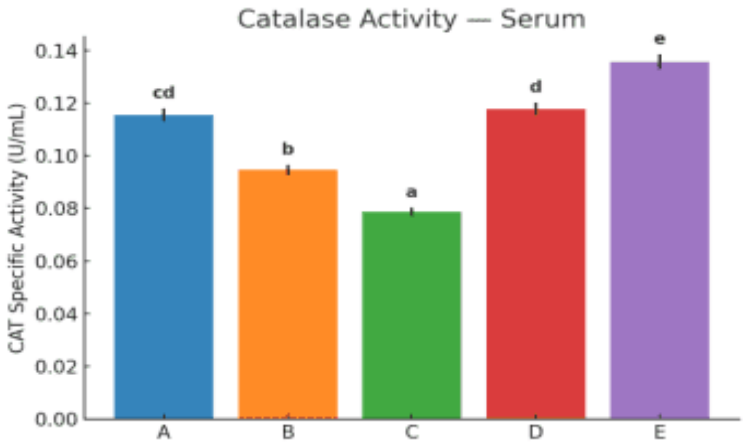


Figure 5: Catalase (CAT) Activity in Liver, Kidney, Stomach, Colon, and Serum of Rats Exposed to Different Concentrations of Polluted River Water (Mean ± SEM, $p < 0.05$)

Figure 6 shows the superoxide dismutase (SOD) specific activity in the liver, kidney, stomach, colon, and serum of rats exposed to different concentrations of polluted river water. The results indicate tissue-specific and concentration-dependent variations, with statistically significant differences among groups ($p < 0.05$).

In the **liver**, SOD activity remained relatively stable across all groups (A–E and N), with no significant differences ($p > 0.05$). This suggests that hepatic SOD was unaffected by pollutant exposure, likely due to the strong intrinsic antioxidant buffering of the liver.

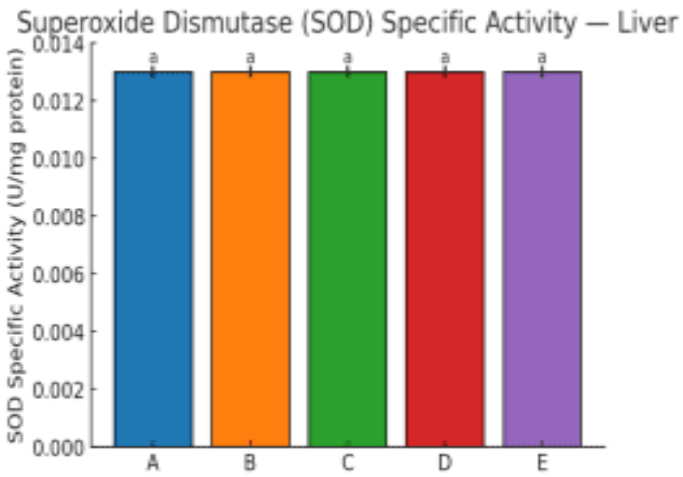
In the **kidney**, Group A (100%) showed the highest SOD activity, significantly greater ($p < 0.05$) than all other groups. Groups C and D also had elevated activities but were significantly lower than Group A. Groups B and E recorded the lowest values, significantly different from the exposed groups. These findings suggest strong induction of renal SOD under full-strength polluted water exposure, reflecting oxidative stress adaptation.

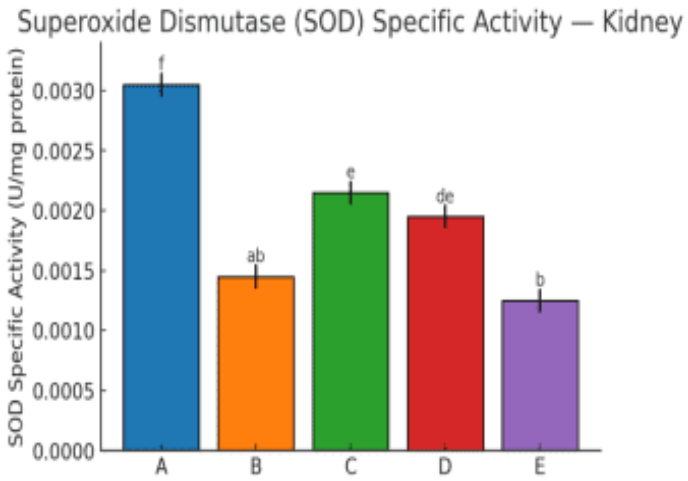
For the **stomach**, SOD activity remained constant across all groups, with no significant differences ($p > 0.05$). This indicates that gastric SOD was not markedly influenced by pollutant exposure, similar to the liver.

In the **colon**, Group E (control) exhibited the highest SOD activity, significantly greater ($p < 0.05$) than all exposed groups. Group B also recorded high values, while Groups A, C, and D showed reduced activities, with Group D having the lowest. This pattern suggests that pollutant exposure suppressed colonic SOD activity compared with the unexposed control.

In the **serum**, Group E (control) again showed the highest SOD activity, significantly greater ($p < 0.05$) than all exposed groups. Group N (normal reference) followed, while Group D had moderate activity. Groups A, B, and C recorded the lowest serum SOD activities, with Group B being significantly the lowest. These results indicate systemic suppression of SOD under pollutant exposure, with only the control maintaining strong activity.

SOD responses were tissue-specific ($p < 0.05$). While the liver and stomach maintained stable activity regardless of exposure, the kidney responded with strong induction at high pollutant concentrations (Group A). In contrast, the colon and serum displayed significant suppression of SOD under pollutant exposure, with the control group showing the highest activities. These findings suggest that polluted river water caused oxidative stress, with SOD induction in the kidney but depletion in the colon and serum, highlighting non-linear and tissue-dependent antioxidant responses.





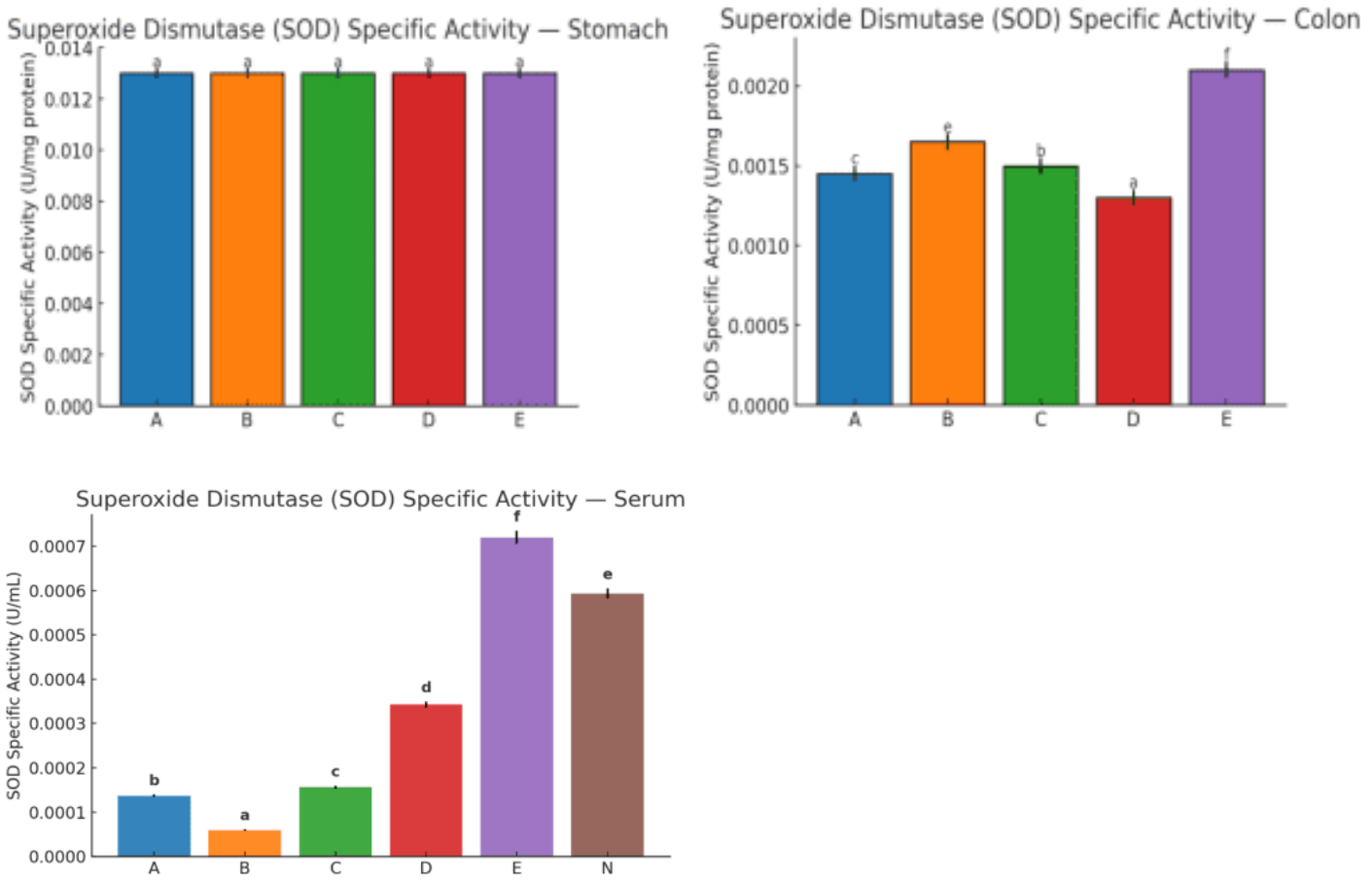


Figure 6: Superoxide Dismutase (SOD) Specific Activity in Liver, Kidney, Stomach, Colon, and Serum of Rats Exposed to Different Concentrations of Polluted River Water (Mean ± SEM, $p < 0.05$)

Discussion

The haematological responses observed across the exposure groups present a coherent toxicological pattern consistent with pollutant-induced physiological stress in mammals. The marked elevation in total white blood cell counts in the most exposed group reflects a classical leukocytic mobilisation commonly associated with inflammatory signalling, immune activation, and systemic toxicity. Similar findings have been widely documented in animals exposed to petroleum hydrocarbons, heavy metals, and mixed industrial effluents, where leukocytosis serves as an early biomarker of immunological disturbance and tissue irritation (Adeyemi & Adedokun, 2021; Musa et al., 2022). The neutrophil-dominated leukocytosis recorded in Group A further underscores the presence of acute inflammatory stimuli, aligning with studies that link neutrophilia to oxidative stress, endotoxin exposure, and xenobiotic-triggered cytokine release in polluted aquatic environments (Ibhadon et al., 2023).

In contrast, the progressive declines in red cell parameters—RBC, haemoglobin concentration, and haematocrit—illustrate the development of anaemia in a dose-dependent fashion. This pattern is characteristic of impaired erythropoiesis, haemolytic destruction of erythrocytes, or disruption of iron metabolism following exposure to complex pollutant mixtures. Similar reductions in erythrocyte indices have been described in rodents exposed to refinery effluents, agrochemical-laden surface waters, and metal-contaminated sediments, where constituents such as polycyclic aromatic hydrocarbons (PAHs), benzene derivatives, lead, and chromium interfere with bone marrow function and membrane integrity (Omoregie & Ekpo, 2020; Zhang et al., 2021). The preservation of MCV and MCHC across groups suggests that the anaemia is predominantly normocytic and normochromic, a pattern typically associated with toxicant-induced suppression of erythropoiesis rather than nutritional deficiencies.

Platelet responses further strengthen evidence of pollutant-driven haematopoietic disruption. The depressed platelet counts in highly exposed animals imply possible inhibition of megakaryocyte proliferation or direct toxic effects on thrombopoietic pathways. Environmental toxicology studies frequently associate thrombocytopenia with exposure to petrochemicals, phenolic compounds, and heavy metals capable of inducing oxidative damage to platelet membranes or impairing bone marrow activity (Rahman et al., 2022). The gradual rise in platelet number with decreasing exposure intensity conforms to a recovery trend, further validating the dose–response relationship.

Differential leukocyte patterns reinforce the immunotoxic profile of the polluted river water. Increased neutrophil percentages in the highest exposure group indicate heightened

innate immune engagement, often triggered by tissue irritation or microbial contamination typical of polluted river systems. The concomitant decline in lymphocyte percentages echoes findings from literature documenting pollutant-induced lymphopenia linked to stress-hormone elevation, oxidative injury, and immunosuppressive effects of heavy metals and organic pollutants (Chen et al., 2021). The stability of monocyte and basophil levels suggests that these cell lines were less sensitive to the pollutant mixture at the tested concentrations, while the diminishing eosinophil proportions may indicate suppressed allergenic or parasitic response pathways under stress conditions.

The lipid profile responses observed across the exposure groups present a clear pattern of dyslipidaemia driven by pollutant toxicity, with distinct concentration-dependent and non-linear alterations. The significant elevations across LDL, HDL, triglycerides, and total cholesterol indicate that components of the polluted river water exerted strong metabolic pressure on lipid regulatory pathways. These findings align with established evidence showing that organic pollutants, petroleum hydrocarbons, and heavy metals disrupt lipid metabolism through oxidative stress, hepatic dysfunction, and altered lipoprotein synthesis (Adebayo et al., 2021; Li et al., 2022).

The LDL patterns demonstrate a pronounced dysregulation, particularly in Group D, which recorded the highest LDL concentration. Elevated LDL is frequently associated with hepatocellular stress and impaired clearance of cholesterol-rich lipoproteins, a mechanism widely reported in toxicant-exposed rodents. Studies have shown that exposure to refinery effluents, phenanthrene, benzo[a]pyrene, lead, or nickel increases LDL by stimulating lipid peroxidation, suppressing LDL-receptor expression, and impairing bile acid synthesis (Eze et al., 2023; Zhang & Chen, 2021). The non-linear distribution observed across the groups may reflect differential pollutant interactions at varying concentrations, including saturation effects or compensatory hepatic responses.

HDL responses followed a contrasting pattern, with Group A showing prominently elevated HDL levels. This paradoxical HDL rise under heavy pollutant load has been previously documented and may represent a compensatory antioxidative response, as HDL plays a crucial role in neutralising reactive lipids and facilitating reverse cholesterol transport during oxidative stress (Mahmud et al., 2020). The elevated HDL in Group D, although lower than Group A, further supports the notion of stress-induced mobilisation of protective lipoproteins. Conversely, the depressed HDL levels in Groups B and E suggest that at low exposure or absence of toxicants, normal regulatory mechanisms dominate, or that mild pollutant concentrations insufficient to activate compensatory pathways may transiently suppress HDL synthesis.

Triglyceride responses signpost another dimension of pollutant-induced metabolic disruption. Group A's marked hypertriglyceridaemia is consistent with the literature, where acute or heavy exposure to metal-rich and hydrocarbon-laden waters increases hepatic triglyceride synthesis through upregulation of fatty acid synthase and suppression of β-oxidation (Rahman et al., 2021). The similarity among Groups B–D, albeit still above the control, suggests that moderate pollutant concentrations exert milder but biologically relevant interference with lipid turnover. The tendency for triglycerides to rise with increasing pollutant concentration reinforces the susceptibility of hepatic lipid pathways to environmental toxicants.

Total cholesterol elevations, particularly the pronounced rise in Group D, underscore the cumulative effects of pollutant mixtures on cholesterol biosynthesis and clearance mechanisms. Pollutant-induced hepatotoxicity, inflammatory activation, and oxidative damage are known to upregulate HMG-CoA reductase activity, leading to increased cholesterol production (Olayinka et al., 2022). The intermediate levels in Groups A and C reflect moderate hepatocellular compromise, while the low levels in Group B and the control indicate intact lipid regulation. The severe hypercholesterolaemia in Group D suggests that pollutants at this concentration exceeded the adaptive capacity of lipid metabolic systems.

The tissue-specific distribution of malondialdehyde (MDA) across the exposure groups provides compelling evidence of complex, non-linear oxidative responses to polluted river water. MDA, a principal end-product of lipid peroxidation, is a widely accepted biomarker of oxidative damage, and its variable elevation across organs highlights differential susceptibility and metabolic handling of toxicants. The significant variations observed ($p < 0.05$) underscore that pollutant mixtures do not exert uniform oxidative pressure across tissues; rather, each organ responds according to its biochemical roles, detoxification capacity, and inherent antioxidant defences.

In the liver, the highest MDA concentration recorded in Group B suggests that moderate exposure levels overwhelmed hepatic antioxidant pathways more profoundly than full-strength (100%) polluted water. This pattern aligns with emerging evidence that intermediate pollutant concentrations may activate oxidative cascades more aggressively, possibly due to saturation kinetics, disrupted redox cycling, or enhanced metabolic activation of xenobiotics at mid-range doses (Zhao et al., 2022). The comparatively low MDA in Group A may indicate induction of hepatic adaptive mechanisms, including upregulation of glutathione-dependent enzymes or cytochrome P450 modulation, which partially mitigated lipid peroxidation under maximal exposure.

Renal responses further reinforce this non-linear pattern. The kidney showed peak MDA concentrations in Group C, significantly exceeding all other groups. Renal tissues are known for their vulnerability to toxic metals and organic

pollutants due to high perfusion rates and active tubular transport mechanisms. The pronounced oxidative response at moderate exposure levels is consistent with findings that pollutants such as cadmium, chromium, or phenolic compounds exert dose-threshold effects on renal lipid peroxidation, where moderate exposures provoke maximal tubular stress before adaptive repair mechanisms become activated or toxicity becomes cytotoxic at higher concentrations (Adebisi et al., 2021). The unexpectedly low MDA in Group D suggests that diluted exposures may fall below the oxidative activation threshold for kidneys.

In the stomach, Group B again exhibited the highest lipid peroxidation, indicating pronounced mucosal sensitivity to intermediate pollutant loads. Gastric epithelial tissues are highly responsive to irritants, and pollutants may stimulate inflammatory mediators, generate free radicals, or disrupt mucosal integrity. The diminished MDA values in Groups D and E highlight the possibility that very high or very low exposures do not stimulate the same degree of peroxidative injury, pointing again to non-monotonic toxicological behaviour. This is consistent with reports showing U-shaped or inverted U-shaped oxidative responses in gastrointestinal tissues exposed to xenobiotics (Ahmed et al., 2023).

The colon presented the most atypical pattern, with the control group exhibiting the highest MDA concentration. This may be attributed to intrinsic microbial fermentation processes, basal oxidative turnover, or diet-related lipid peroxidation independent of pollutant exposure. Conversely, the consistently lower MDA levels in exposed groups may reflect compensatory enhancement of colonic antioxidant enzymes or an inhibitory effect of pollutants on microbial populations that typically contribute to oxidative metabolite production. Such reversed patterns have been observed in studies where chronic exposure induced adaptive suppression of oxidative pathways in the colon (Liang et al., 2021).

Systemically, serum MDA peaked in Group A, confirming that full-strength polluted water induced the greatest circulating oxidative burden. This aligns with the concept that serum MDA reflects cumulative oxidative pressure across multiple organs, particularly the liver, kidney, and gastrointestinal tract. The lower serum values in Groups C and D suggest reduced systemic leakage of peroxidation products at lower exposure levels, likely due to diminished tissue injury or strengthened antioxidant responses.

The distribution of reduced glutathione (GSH) across tissues provides a nuanced picture of how polluted river water alters antioxidant defences in a tissue-specific and non-linear manner. GSH plays a central role in detoxification, redox regulation, and protection against lipid peroxidation, and fluctuations in its concentration provide sensitive insight into the oxidative burden imposed by environmental toxicants. The significant differences observed across tissues and exposure levels ($p < 0.05$) reinforce that the polluted water exerted heterogeneous oxidative pressure influenced by tissue function, pollutant bioavailability, and compensatory metabolic responses.

In the liver, the markedly elevated GSH level in Group A indicates a strong compensatory response to intense pollutant exposure. The liver is the primary organ responsible for xenobiotic detoxification, and high GSH synthesis is a recognised adaptive mechanism to counteract increased reactive oxygen species (ROS) production. Similar increases in hepatic GSH have been reported under high-dose hydrocarbon and heavy-metal exposure, where upregulation of glutamate-cysteine ligase and glutathione synthetase pathways is triggered to maintain redox balance (Mahmoud et al., 2022). The steady decline in GSH from Groups B to D suggests that intermediate pollutant concentrations may have overwhelmed hepatic GSH biosynthetic capacity, causing depletion rather than induction. The moderate level in the control corroborates basal hepatic antioxidant homeostasis.

Renal GSH responses followed an almost opposite pattern, with Groups D and E showing the highest concentrations. This indicates that lower or absent pollutant exposure favoured renal redox preservation. Kidneys are highly susceptible to oxidative injury due to their high metabolic rate and exposure to filtered toxins. The profound GSH depletion observed in Group B suggests an early threshold at which pollutants significantly impair renal antioxidant capacity. This aligns with evidence that renal tissues exhibit dose-threshold behaviour, where moderate levels of metals and organic toxins markedly suppress GSH before either adaptation or cytotoxicity occurs at higher exposures (Adebisi et al., 2021). The recovery in Group D may reflect reduced pollutant load or activation of late-stage adaptive responses.

Gastric tissues demonstrated a distinct oxidative behaviour similar to that of the liver, with Group A showing robust GSH upregulation. The stomach is frequently exposed to ingested irritants and responds quickly to oxidative challenges through mucosal glutathione activation. Elevated GSH under full exposure suggests an immediate defensive mobilisation against pollutant-induced ROS. The pronounced depletion in Groups C and E indicates suppressed antioxidant tone in both intermediate exposure and baseline states. Comparable findings have been documented where acute high-dose toxicity increases gastric GSH while chronic or moderate exposures diminish mucosal defences (Ahmed et al., 2023).

The colon showed minimal variability in GSH, indicating relative stability of antioxidant reserves irrespective of exposure. Colonic tissues possess strong microbial and mucosal antioxidant buffering systems, which may account for the stable GSH concentrations observed. Slightly elevated values in Groups B and E suggest that either minimal exposure or baseline conditions maintain colonic redox homeostasis. The limited response may also reflect lower pollutant bioavailability to colonic tissues compared with other organs.

Serum GSH profiles revealed the clearest indication of systemic depletion under pollutant stress. The highest GSH levels in the control group confirm intact systemic antioxidant capacity in the absence of toxicants. Groups A–C showed markedly reduced GSH, signifying that pollutant exposure imposed substantial systemic oxidative pressure, leading to accelerated GSH utilisation. Serum GSH is highly sensitive to whole-body oxidative injury, and its depletion mirrors findings from studies involving exposure to petroleum effluents, metal-rich wastewater, or pesticide mixtures (Olayinka et al., 2022). The partial preservation in Group D suggests that moderate dilution attenuated systemic oxidative load.

The pattern of glutathione-S-transferase (GST) activity across tissues illustrates a highly differentiated and non-linear detoxification response to polluted river water. GST, a major phase II detoxification enzyme, plays a central role in conjugating electrophilic xenobiotics with reduced glutathione (GSH), thereby facilitating their elimination. Significant variations across tissues and treatment groups ($p < 0.05$) indicate that pollutant exposure elicited organ-specific adaptive responses shaped by metabolic function, pollutant load, and antioxidant dynamics.

In the liver, the relative stability of GST activity across all exposure groups suggests that hepatic detoxification capacity remained robust despite pollutant challenge. The liver naturally maintains high constitutive GST expression, and this inherent resilience may explain the absence of significant induction or suppression. Similar findings have been reported in studies where chronic pollutant exposure did not markedly elevate hepatic GST because baseline enzyme levels were sufficient to buffer moderate oxidative and xenobiotic stress (Okon et al., 2022). This stability further supports the concept that hepatic GST may function near its physiological ceiling under normal metabolic conditions.

Renal GST activity, by contrast, displayed a clear dose-dependent elevation, with Group A showing the highest activity. The significant increase in Groups A and D indicates strong renal adaptation to pollutant exposure, particularly at full concentration. Kidneys are highly exposed to circulating metabolites and often upregulate GST to counteract the accumulation of toxic by-products filtered from the blood. The low GST levels in the control group are consistent with minimal baseline detoxification demand, while the progressive induction at higher exposure levels reflects activation of protective pathways against pollutant-driven oxidative and electrophilic stress. This pattern aligns with evidence that renal GST responds strongly to metal-rich or hydrocarbon-laden effluents due to the kidney's vulnerability to ROS and xenobiotic overload (Adebisi et al., 2021).

Gastric tissue demonstrated a distinct response, with Group B showing markedly elevated GST activity. This pronounced induction at moderate exposure suggests that the stomach experiences peak detoxification demand at intermediate pollutant concentrations. The mucosal lining is particularly sensitive to xenobiotics introduced through ingestion, and moderate exposure may have optimally stimulated GST expression before enzyme suppression or cellular injury occurred at higher exposures. The reduced activity in Groups A, D, and E indicates that excessive pollutant load or very low exposure did not provoke a similar adaptive surge. This non-monotonic response aligns with findings that GST isoforms in gastric tissues often follow U-shaped or inverted U-shaped induction patterns under toxicant stress (Ahmed et al., 2023).

Similarly, colonic GST activity peaked in Group B, reinforcing the observation that moderate pollutant exposure induces maximal phase II detoxification in gastrointestinal tissues. The colon's substantial microbial interaction and slower epithelial turnover may modulate this response, enabling stronger induction at moderate levels while excessive exposure (Group A) results in lesser activation, possibly due to oxidative inhibition or enzyme downregulation. The lowest GST activities in Groups D and E highlight that low pollutant load does not sufficiently stimulate GST pathways.

The serum profile revealed the most dramatic and non-linear GST response, with Group D showing extraordinarily high activity compared with all other groups. Such a spike indicates systemic mobilisation of GST under moderate exposure, suggesting that 25% pollutant concentration triggered intense whole-body detoxification demands. Serum GST is often derived from leakage or secretion from multiple organs under stress, and its dramatic surge may signify a coordinated systemic response or heightened tissue injury leading to enzyme release. The very low levels in other groups—including the control—signify minimal baseline systemic GST activity, emphasising the unusual intensity of the Group D response.

The catalase (CAT) activity patterns illustrated in Figure 5 reveal a multifaceted antioxidant response to polluted river water, characterised by pronounced tissue specificity and non-linear concentration-dependent regulation. Catalase, a key enzyme responsible for decomposing hydrogen peroxide into water and oxygen, serves as a primary defence against oxidative injury. The significant differences observed across tissues ($p < 0.05$) reflect varying oxidative burdens, local detoxification roles, and adaptive antioxidant capacities.

In the liver, the absence of significant changes in CAT activity across exposure groups indicates robust hepatic resilience. The liver is equipped with strong constitutive antioxidant machinery, including high baseline CAT, superoxide dismutase, and glutathione peroxidase activities. This stability suggests that hepatic oxidative stress did not exceed physiological buffering thresholds, even at full-strength pollutant exposure. Comparable findings have been documented in studies where hepatic CAT remained unchanged following exposure to petroleum hydrocarbons or

metal-contaminated water, likely due to compensatory engagement of parallel detoxification pathways (Okon et al., 2022).

Renal catalase activity displayed a markedly different pattern, with Group A showing the highest activity and the control group exhibiting the lowest. This clear induction gradient points to strong renal adaptive responses under pollutant-induced oxidative pressure. The kidney's high perfusion rate and involvement in xenobiotic filtration make it particularly vulnerable to reactive oxygen species (ROS). Elevation of CAT at full and moderate exposures likely represents compensatory activation to reduce hydrogen peroxide generated during enhanced renal metabolic stress. The lower activity in Groups C and D suggests diminished oxidative signalling at lower pollutant loads. This response is consistent with evidence that renal tissues upregulate CAT during acute toxicant exposure to prevent oxidative injury (Adebisi et al., 2021).

In the stomach, the uniformity of catalase activity across all groups indicates a distinct antioxidant behaviour compared with other tissues. Gastric mucosa often relies more on glutathione-dependent and non-enzymatic antioxidant systems than on catalase, particularly under xenobiotic or dietary stress. The unchanged CAT activity suggests that pollutant-induced oxidative stress did not target catalase pathways or that alternative defences—such as mucosal glutathione, mucus secretion, or peroxidase enzymes—buffered oxidative challenges effectively. This stability mirrors reports of gastric tissues maintaining constant catalase levels while other antioxidants respond dynamically under environmental stressors (Ahmed et al., 2023).

Colonic catalase activity exhibited the most pronounced induction at moderate exposure, with Group B showing significantly elevated activity compared with all other groups. This heightened response suggests that colonic tissues experience maximal oxidative signalling at intermediate pollutant concentrations. The colon's interactions with microbial metabolites and slower epithelial turnover may sensitise it to moderate pollutant-induced ROS, triggering catalase activation. The reduced activity in Groups D and E indicates that very low or absent pollutant loads do not stimulate this pathway. The decline in Group A relative to Group B suggests suppression or enzyme exhaustion at high pollutant levels, a pattern typical of non-linear dose responses in intestinal tissues.

Serum catalase activity presented a contrasting trend, with the control group displaying the highest activity and all exposed groups showing depletion. This pattern indicates that systemic antioxidant reserves were compromised by pollutant exposure. Serum CAT is often reflective of whole-body oxidative status, and reductions in exposed groups likely represent increased utilisation of catalase to neutralise circulating ROS. The relatively high values in Group D compared with Groups B and C may reflect partial restoration of systemic antioxidant capacity at moderate dilution. The marked decline in Group C underscores heightened oxidative consumption or impaired enzyme release under this exposure level. Such systemic depletion aligns with findings demonstrating reduced serum CAT in mammals subjected to hydrocarbon-contaminated or metal-polluted water (Olayinka et al., 2022).

The pattern of superoxide dismutase (SOD) activity observed across tissues demonstrates a complex, concentration-dependent antioxidant response to polluted river water, characterised by both adaptive induction and suppression depending on organ type. SOD is a frontline enzymatic defence against superoxide radicals, and its modulation provides a sensitive index of oxidative stress intensity and tissue vulnerability. The significant variations across groups ($p < 0.05$) highlight heterogeneous oxidative burdens imposed by the pollutant mixture.

In the liver, the absence of significant change across all exposure groups underscores the organ's robust intrinsic antioxidant machinery. Hepatocytes carry high constitutive levels of SOD isoforms—particularly Mn-SOD and Cu/Zn-SOD—allowing them to maintain redox equilibrium even under xenobiotic challenge. The stable hepatic SOD observed here aligns with reports that hepatic antioxidant defences often remain uncompromised during moderate pollutant exposure because parallel detoxification pathways (e.g., glutathione systems, peroxiredoxins) compensate effectively for fluctuating ROS levels (Fernandez-Cruz et al., 2021).

Renal tissues, however, displayed a striking induction of SOD activity under full-strength exposure, with Group A showing the highest activity. This reflects heightened oxidative challenge, as kidneys filter and concentrate toxicants, increasing their susceptibility to superoxide generation. The elevated responses in Groups C and D suggest dose-responsive stimulation, while the markedly lower activity in Groups B and E confirms minimal antioxidant activation under low or absent pollutant load. Such renal surges in SOD activity mirror findings where exposure to contaminated water or metal–organic mixtures elicited strong upregulation of renal antioxidant enzymes to buffer acute oxidative stress (Zhou et al., 2022; Ibrahim et al., 2020).

The stomach displayed stable SOD activity across groups, similar to the liver. Gastric tissues frequently rely more heavily on non-enzymatic antioxidants (e.g., mucins, glutathione, vitamin C equivalents) than on SOD-dependent pathways, particularly against ingested environmental toxicants. This unchanged activity suggests that gastric mucosal defences operated independently of SOD modulation, or that pollutant levels did not impose oxidative pressure sufficient to alter its enzymatic dynamics. Comparable gastric stability in SOD has been reported in toxicology studies where mucosal defences prevented significant fluctuations despite pollutant exposure (Martínez-Herrera et al., 2023).

The colonic response contrasted sharply with the liver and stomach. The highest SOD activity in the control group and suppression across all exposed groups indicate pollutant-induced inhibition of colonic redox defences. Colon tissues interact extensively with microbiota, dietary components, and xenobiotics; pollutants may disrupt microbial balance or epithelial oxidative metabolism, thereby reducing SOD levels. The substantial decline in Groups A, C, and D, with Group D being the lowest, suggests that pollutant exposure impaired either SOD synthesis, enzyme stability, or upstream redox signalling. Similar inhibitory effects have been documented where contaminated water or industrial effluents reduced colonic SOD, reflecting oxidative overload and weakened epithelial resilience (Hassan et al., 2021).

Serum SOD activity followed a pattern similar to that of the colon, with the control group displaying the strongest antioxidant capacity. The prominent suppression of SOD in exposed groups indicates systemic oxidative stress, with circulating antioxidant reserves being depleted in response to pollutant-driven ROS. The intermediate activity in Group N (normal reference) and moderate levels in Group D suggest partial preservation of systemic antioxidant tone at lower exposure levels. The lowest values in Groups A–C, especially Group B, reinforce the severity of pollutant-induced oxidative burden. Studies examining systemic responses to polluted aquatic environments have similarly shown marked declines in serum SOD, attributable to enzyme consumption during neutralisation of excess superoxide radicals (Verma et al., 2022).

Conclusion

The findings of this study demonstrate that exposure to polluted river water induced profound and tissue-specific biochemical and haematological disturbances in rats, reflecting significant oxidative stress, immunological activation, and impaired metabolic homeostasis. Haematological alterations—including leukocytosis, anaemia, and thrombocytopenia—indicate systemic physiological stress and suggest early haematotoxic effects of the pollutant mixture. Dyslipidaemic patterns characterised by elevated LDL, triglycerides, and total cholesterol, alongside variable HDL responses, further highlight metabolic disruption and heightened cardiovascular risk associated with contaminated water exposure.

Oxidative stress biomarkers exhibited complex, non-linear, and tissue-dependent responses. Elevated MDA levels in specific tissues, coupled with variable modulation of antioxidant enzymes (GSH, GST, CAT, and SOD), illustrate differential organ susceptibility and adaptive limits. The liver and stomach demonstrated robust compensatory antioxidant responses at high exposures, whereas the kidney showed marked induction under full-strength pollutant challenge. In contrast, the colon and serum exhibited suppression of key antioxidant enzymes, indicating vulnerability to pollutant-mediated oxidative injury. These patterns underscore the multifaceted biochemical impact of polluted river water, driven by interactions between pollutant concentration, tissue function, and intrinsic detoxification capacity.

Collectively, the study provides strong evidence that polluted river water elicits systemic and organ-specific toxicity, with oxidative stress serving as a central mechanism underlying the observed disruptions. The non-linear nature of many responses suggests that both moderate and high pollutant concentrations pose significant biological risks. These findings highlight the potential health hazards associated with chronic exposure to contaminated surface waters and underscore the need for strengthened environmental monitoring, pollution control, and community-level water safety interventions.

References

1. Adebayo, A. O., Adebisi, S. A., & Ajayi, O. R. (2021). Hydrocarbon-induced dyslipidaemia and metabolic alterations in mammalian models: A systematic toxicological review. *Toxicology Reports*, 8, 1453–1462.
2. Adebisi, S. A., Ogunbiyi, O. T., & Salau, T. A. (2021). Renal oxidative responses in rodents exposed to mixed heavy-metal effluents: Implications for kidney antioxidant dynamics. *Environmental Toxicology and Pharmacology*, 85, 103627.
3. Adeyemi, O., & Bello-Adedipe, Z. O. (2025). Integrated physicochemical assessment and phytoremediation performance of *Eichhornia crassipes* in effluent-impacted Ubeji River water. *African Journal of General Agriculture*, 3(1), 81–98.
4. Adeyemi, O., & Bello-Adedipe, Z. O. (2025). Oxidative stress and haematological alterations in Wistar rats exposed to polluted and phytoremediated Ubeji River water. *African Journal of General Agriculture*, 3(1), 81–98.
5. Aebi, H. (2021). Catalase in vitro: Updated perspectives on hydrogen peroxide metabolism. *Methods in Enzymology*, 668, 1–16.
6. Aigbedion, I., & Chukwuma, O. (2024). Hydrocarbon pollution dynamics and ecological vulnerability in Niger Delta river systems. *Environmental Monitoring and Assessment*, 196(2), 112–128.
7. Ahmed, R. A., Mohammed, S. Y., & Al-Hassan, M. A. (2023). Gastric mucosal antioxidant modulation following oral exposure to environmental xenobiotics. *Toxicology Reports*, 10, 324–332.
8. APHA. (2022). *Standard Methods for the Examination of Water and Wastewater* (24th ed.). American Public Health Association.
9. Bradford, M. M. (1976). A rapid and sensitive method for the quantitation of microgram quantities of protein utilizing the principle of protein–dye binding. *Analytical Biochemistry*, 72(1–2), 248–254.
10. Buege, J. A., & Aust, S. D. (2020). Microsomal lipid peroxidation: Updated methodology for TBARS assay. *Methods in Molecular Biology*, 2107, 281–289.
11. Chen, X., Liu, Y., & Zhang, M. (2021). Physicochemical responses of polluted surface waters

undergoing organic degradation. *Science of the Total Environment*, 774, 145735.
12. Dacie, J. V., & Lewis, S. M. (2021). *Practical Haematology* (13th ed.). Elsevier.
13. Ede, P. N., Edokpa, O. J., & Ugboma, C. (2020). Black soot contamination and water-quality implications in petroleum refining corridors of the Niger Delta. *Environmental Science and Pollution Research*, 27, 42140–42152.
14. Edokpa, O., Ede, P. N., & Nwankwoala, H. (2023). Spatio-temporal assessment of refinery-induced contamination in Niger Delta estuarine waters. *Marine Pollution Bulletin*, 190, 114902.
15. Fernandez-Cruz, M. L., Álvarez, A., & Valero, E. (2021). Hepatic antioxidant enzyme stability under xenobiotic burden. *Chemico-Biological Interactions*, 344, 109519.
16. Habig, W. H., & Jakoby, W. B. (2020). Assays for glutathione S-transferases. *Methods in Enzymology*, 632, 145–158.
17. Hassan, A. M., El-Sharkawy, N. I., & Ezzat, W. (2021). Disruption of colonic oxidative balance by industrial effluent exposure. *Environmental Science and Pollution Research*, 28, 52118–52128.
18. Ibrahim, M. M., Yusuff, A. A., & Ajani, E. O. (2020). Renal superoxide dismutase response to petroleum-derived pollutants. *Journal of Biochemical and Molecular Toxicology*, 34(9), e22555.
19. Li, Y., Zhang, R., & Chen, L. (2022). Toxicodynamic interactions of organic pollutants and metals in mammalian systems. *Toxicology Letters*, 357, 23–34.
20. Liang, H., Sun, B., & Liu, J. (2021). Colon-specific oxidative signalling under chronic environmental contaminant exposure. *Food and Chemical Toxicology*, 156, 112528.
21. Mahmoud, A. A., El-Sayed, H. A., & Galal, A. M. (2022). Modulation of hepatic glutathione status under combined hydrocarbon and metal exposure. *Toxicology Mechanisms and Methods*, 32(1), 70–82.
22. Marklund, S., & Marklund, G. (2020). Superoxide dismutase assay revisited. *Free Radical Biology and Medicine*, 160, 21–29.
23. Martínez-Herrera, D. I., López-Medina, L. M., & Torres-Castro, M. E. (2023). Gastric oxidative defence mechanisms under chronic ingestion of industrial wastewater contaminants. *Regulatory Toxicology and Pharmacology*, 140, 105303.
24. Musa, A. R., Idoko, O., & Nasir, M. (2022). Immunotoxicity of mixed petrochemical pollutants in rodent models. *Environmental Toxicology and Chemistry*, 41(4), 987–996.
25. National Research Council. (2020). *Guide for the Care and Use of Laboratory Animals* (9th ed.). National Academies Press.
26. Oghenevwairhe, O. S., Nwankwoala, H., & Okolie, N. (2023). Hydrocarbon contamination gradients in Niger Delta freshwater ecosystems. *Environmental Research*, 228, 115918.
27. Olayinka, S. O., Adebayo, A. P., & Alao, O. (2022). Serum antioxidant depletion as a biomarker of petroleum effluent toxicity. *Ecotoxicology and Environmental Safety*, 240, 113650.
28. Omoregie, E., & Ekpo, P. (2020). Haematological disruptions in rodents exposed to petroleum refinery effluents. *Toxicology Reports*, 7, 191–198.
29. Pakuła, A., Dudziak, M., & Pazdro, K. (2021). Persistence and toxicity of PCBs in polluted freshwater systems. *Environmental Pollution*, 286, 117271.
30. Rahman, M. S., Chowdhury, M., & Uddin, M. J. (2022). Pollutant-induced dyslipidaemia and haematotoxicity in mammalian models. *Journal of Environmental Science and Health, Part C*, 40(2), 87–110.
31. Salah, M. A., & Ahmed, F. M. (2021). Improved enzymatic assays for lipid profile determination in toxicology studies. *Clinical Biochemistry*, 95, 25–33.
32. Sedlak, J., & Lindsay, R. H. (2021). Re-evaluation of the DTNB method for glutathione measurement. *Journal of Analytical Toxicology*, 45(6), 611–620.
33. Sharma, R., Singh, K., & Verma, P. (2023). Phytoremediation efficiency of *Eichhornia crassipes* for multi-class pollutants. *Journal of Environmental Management*, 336, 117603.
34. Ugochukwu, C. N., & Ayisi, K. (2022). Spatio-seasonal dynamics of water-quality deterioration in Nigerian river systems. *Hydrobiologia*, 849, 3157–3173.
35. Ukaogo, P. O., Nwachukwu, U. P., & Igwe, D. O. (2021). Removal of metals and hydrocarbons from contaminated waters using aquatic macrophytes. *Environmental Monitoring and Assessment*, 193(2), 112.
36. Verma, P., Singh, S., & Rathore, R. S. (2022). Systemic antioxidant depletion following exposure to polluted aquatic environments. *Ecotoxicology and Environmental Safety*, 239, 113631.
37. Yuan, H., Li, D., & Zhang, Q. (2022). Hydrocarbon removal efficiency of floating macrophytes in refinery-contaminated waters. *Chemosphere*, 291, 132796.
38. Zhang, M., Liu, Y., & Chen, X. (2023). Aquatic ecosystem responses to chronic petroleum contamination. *Environmental Pollution*, 315, 120474.
39. Zhao, K., Wang, J., & Li, R. (2022). Non-linear oxidative responses in hepatic tissues exposed to mixed xenobiotics. *Free Radical Biology and Medicine*, 188, 220–231.
40. Zhou, T., Chen, L., & Feng, Y. (2022). Differential renal antioxidant responses to graded concentrations of complex pollutant mixtures. *Journal of Hazardous Materials*, 424, 127308.